1   **Short Title:** Monocot ELF3 functions in dicots

2

3

4

5

6

7   **Corresponding Author:**

8

9   Dmitri A. Nusinow, Ph.D.

10   Assistant Member

11   Danforth Plant Science Center

12   975 N. Warson Rd.- Room 3030

13   St. Louis, MO 63132

14   (314)587-1489

15   meter@danforthcenter.org

16

Cross-species complementation reveals conserved functions for EARLY FLOWERING 3 between monocots and dicots

He Huang, Malia A. Gehan, Sarah E. Huss, Sophie Alvarez[2], Cesar Lizarraga, Ellen L. Gruebbling, John Gierer, Michael J. Naldrett[2], Rebecca K. Bindbeutel, Bradley S. Evans, Todd C. Mockler, and Dmitri A. Nusinow[*]

Donald Danforth Plant Science Center, St. Louis, MO, 63132, USA (H.H., M.A.G., S.A., C.L., J.G., M.J.N., R.K.B., B.S.E., T.C.M., D.A.N.)
Webster University, Webster Groves, MO, 63119, USA (S.E.H.)
Saint Louis University, St. Louis, MO, 63103, USA (E.L.G.)

One Sentence Summary:

Orthologs of a key circadian clock component ELF3 from grasses functionally complement the Arabidopsis counterpart at the molecular and physiological level, in spite of high sequence divergence.

Footnotes:

H.H., M.A.G., T.C.M., and D.A.N. conceived the project; T.C.M., B.S.E. and D.A.N. supervised the experiments; H.H., M.A.G., S.E.H., S.A., C.L., E.L.G., J.G., M.J.N., R.K.B. and D.A.N. performed the experiments; H.H., M.A.G., S.E.H., S.A., C.L., M.J.N. and D.A.N. analyzed the data; H.H., M.A.G., and D.A.N. wrote the manuscript. All authors edited the manuscript.

[2] Present addresses: University of Nebraska-Lincoln, Lincoln, NE, 68588, USA

[*]Corresponding author email: meter@danforthcenter.org

49 **ABSTRACT**

50

51   Plant responses to the environment are shaped by external stimuli and internal signaling

52   pathways. In both the model plant *Arabidopsis thaliana* and crop species, circadian clock factors

53   have been identified as critical for growth, flowering and circadian rhythms. Outside of *A.*

54   *thaliana,* however, little is known about the molecular function of clock genes. Therefore, we

55   sought to compare the function of *Brachypodium distachyon* and *Seteria viridis* orthologs of

56   *EARLY FLOWERING3,* a key clock gene in *A. thaliana.* To identify both cycling genes and

57   putative ELF3 functional orthologs in *S. viridis*, a circadian RNA-seq dataset and online query

58   tool (Diel Explorer) was generated as a community resource to explore expression profiles of

59   *Setaria* genes under constant conditions after photo- or thermo-entrainment. The function of

60   *ELF3* orthologs from *A. thaliana, B. distachyon,* and *S. viridis* were tested for complementation

61   of an *elf3* mutation in *A. thaliana.* Despite comparably low sequence identity versus AtELF3

62   (less than 37%), both monocot orthologs were capable of rescuing hypocotyl elongation,

63   flowering time and arrhythmic clock phenotypes. Molecular analysis using affinity purification

64   and mass spectrometry to compare physical interactions also found that BdELF3 and SvELF3

65   could be integrated into similar complexes and networks as AtELF3, including forming a

66   composite evening complex. Thus, we find that, despite 180 million years of separation, BdELF3

67   and SvELF3 can functionally complement loss of *ELF3* at the molecular and physiological level.

68

69   **INTRODUCTION**

70

71   Plants have developed sophisticated signaling networks to survive and thrive in diverse

72   environments. Many plant responses are shaped, in part, by an internal timing mechanism known

73   as the circadian clock, which allows for the coordination and anticipation of daily and seasonal

74   variation in the environment (Greenham and McClung, 2015). Circadian clocks, which are

75   endogenous oscillators with a period of approximately 24 hours, are critical for regulating the

76   timing of physiology, development, and metabolism in all domains of life (Bell-Pedersen et al.,

77   2005; Doherty and Kay, 2010; Edgar et al., 2012; Harmer, 2009; Wijnen and Young, 2006). In

78   plants and blue-green algae, circadian clocks provide an experimentally observable adaptive

79   advantage by synchronizing internal physiology with external environmental cues (Dodd et al.,

80   2005; Ouyang et al., 1998; Woelfle et al., 2004). Currently, circadian oscillators are best

81   understood in the reference plant *Arabidopsis thaliana*, in which dozens of clock or clock-

82   associated components have been identified using genetic screens and non-invasive, luciferase-

83   based oscillating reporters (Hsu and Harmer, 2014; Nagel and Kay, 2012). These morning-,

84   afternoon-, and evening-phased clock oscillators form multiple interconnected transcription-

85   translation feedback loops and compose a complex network (Hsu and Harmer, 2014; Pokhilko et

86   al., 2012). The *A. thaliana* circadian clock regulates a significant portion of physiology,

87   including photosynthesis, growth, disease resistance, starch metabolism, and phytohormone

88   pathways (Covington et al., 2008; Graf et al., 2010; Harmer et al., 2000; Michael et al., 2008;

89   Wang et al., 2011b), with up to 30% of gene expression under circadian control (Covington et

90   al., 2008; Michael et al., 2008).

91   Within the Arabidopsis clock network, a tripartite protein complex called the evening complex

92   (EC) is an essential component of the evening transcription loop (Huang and Nusinow, 2016b).

93   The EC consists of three distinct proteins, EARLY FLOWERING 3 (ELF3), EARLY

94   FLOWERING 4 (ELF4) and LUX ARRHYTHMO (LUX, also known as PHYTOCLOCK1),

95   with transcript and protein levels peaking in the evening (Doyle et al., 2002; Hazen et al., 2005;

96   Hicks et al., 2001; Nusinow et al., 2011; Onai and Ishiura, 2005). The EC plays a critical role in

97   maintaining circadian rhythms, by repressing expression of key clock genes (Dixon et al., 2011;

98   Helfer et al., 2011; Herrero et al., 2012; Kolmos et al., 2011; Mizuno et al., 2014). Loss-of-

4

99   function mutation of any EC component in *A. thaliana* results in arrhythmicity of the circadian

100 clock and causes excessive cellular elongation and early flowering regardless of environmental

101 photoperiod (Doyle et al., 2002; Hazen et al., 2005; Hicks et al., 2001; Khanna et al., 2003; Kim

102 et al., 2005; Nozue et al., 2007; Nusinow et al., 2011; Onai and Ishiura, 2005).

103

104 In *A. thaliana*, ELF3 directly interacts with ELF4 and LUX, functioning as a scaffold to bring

105 ELF4 and LUX together (Herrero et al., 2012; Nusinow et al., 2011). Additional protein-protein

106 interaction studies and tandem affinity purification coupled with mass spectrometry (AP-MS)

107 have identified many ELF3-associating proteins and established ELF3 as a hub of a complex

108 protein-protein interaction network, which consists of key components from the circadian clock

109 pathway and light signaling pathways (Huang et al., 2016a; Huang and Nusinow, 2016b; Liu et

110 al., 2001; Yu et al., 2008). In this network, ELF3 directly interacts with the major red light

111 photoreceptor phytochrome B (phyB), and CONSTITUTIVE PHOTOMORPHOGENIC 1

112 (COP1), which is an E3 ubiquitin ligase required for proper regulation of photomorphogenesis

113 and also interacts with phyB (Liu et al., 2001; Yu et al., 2008). The physical interaction among

114 ELF3, phyB, and COP1, together with recruitment of direct interacting proteins to the network,

115 provides biochemical evidence for cross-talk between circadian clock and light signaling

116 pathways (Huang and Nusinow, 2016b). Although much work does translate from *A. thaliana* to

117 other plant species, interaction between ELF3 and other proteins have yet to be tested in species

118 outside *A. thaliana*. Whether evening complex-like protein assemblages or a similar ELF3-

119 containing protein-protein interaction network exists in species outside *A. thaliana* is an

120 interesting question to ask.

121

122 Identification and characterization of clock genes in diverse plant species has revealed that many

123 clock components are broadly conserved (Filichkin et al., 2011; Khan et al., 2010; Lou et al.,

124 2012; Song et al., 2010). Furthermore, comparative genomics analysis has found that circadian

125 clock components are selectively retained after genome duplication events, suggestive of the

126 importance of their role in maintaining fitness (Lou et al., 2012). Recently, mutant alleles of

127 *ELF3* were identified associated with the selection of favorable photoperiodism phenotypes in

128 several crops, such as pea, rice, soybean and barley (Faure et al., 2012; Lu et al., 2017;

129   Matsubara et al., 2012; Saito et al., 2012; Weller et al., 2012; Zakhrabekova et al., 2012). These

130   findings are consistent with the reported functions of *A. thaliana* ELF3 in regulating the

131   photoperiodic control of growth and flowering (Hicks et al., 2001; Huang and Nusinow, 2016b;

132   Nozue et al., 2007; Nusinow et al., 2011). However, opposed to the early flowering phenotype

133   caused by *elf3* mutants in *A. thaliana,* pea, and barley (Faure et al., 2012; Hicks et al., 2001;

134   Weller et al., 2012), loss of function mutation of the rice or soybean *ELF3* ortholog results in

135   delayed flowering (Lu et al., 2017; Saito et al., 2012), suggesting ELF3-mediated regulation of

136   flowering varies in different plant species. The molecular mechanisms underlying this difference

137   have not been thoroughly elucidated.

138

139   *Brachypodium distachyon* is a C3 model grass closely related to wheat, barley, oats, and rice.

140   *Setaria viridis*, is a C4 model grass closely related to maize, sorghum, sugarcane, and other

141   bioenergy grasses. Both grasses are small, transformable, rapid-cycling plants with recently

142   sequenced genomes, making them ideal model monocots for comparative analysis with

143   Arabidopsis (Bennetzen et al., 2012; Brutnell et al., 2010). Computational analysis of *B.*

144   *distachyon* has identified putative circadian clock orthologs (Higgins et al., 2010)*,* including

145   *BdELF3*. However, no such comparative analysis has been done systematically in *S. viridis* to

146   identify putative orthologs of circadian clock genes. Therefore, we generated a RNA-seq time-

147   course dataset to analyze the circadian transcriptome of *S. viridis* after either photo- or thermo-

148   entrainment and developed an online gene-expression query tool (Diel Explorer) for the

149   community. We found that the magnitude of circadian regulated genes in *S. viridis* is similar to

150   other monocots after photo-entrainment, but much less after thermal entrainment. We further

151   analyzed the functional conservation of SvELF3, together with previously reported BdELF3, by

152   introducing both ELF3 orthologs into *A. thaliana elf3* mutant for physiological and biochemical

153   characterization. We found that *B. distachyon* and *S. viridis* ELF3 can complement the hypocotyl

154   elongation, flowering time and circadian arrhythmia phenotypes caused by the *elf3* mutation in

155   *A. thaliana.* Furthermore, AP-MS analyses found that *B. distachyon* and *S. viridis* ELF3 were

156   integrated into a similar protein-protein interaction network *in vivo* as their *A. thaliana*

157   counterpart. Our data collectively demonstrated the functional conservation of ELF3 among *A.*

6

158   *thaliana, B. distachyon* and *S. Viridis* is likely due to the association with same protein partners,

159   providing insights of how ELF3 orthologs potentially function in grasses.

160

161   **RESULTS**

162

163   **Identifying and cloning ELF3 orthologs from *B. distachyon* and *S. viridis***

164

165   ELF3 is a plant-specific nuclear protein with conserved roles in flowering and the circadian

166   clock in multiple plant species (Faure et al., 2012; Herrero et al., 2012; Liu et al., 2001; Lu et al.,

167   2017; Matsubara et al., 2012; Saito et al., 2012; Weller et al., 2012; Zakhrabekova et al., 2012).

168   To identify ELF3 orthologs in monocots, we used the protein sequence of *Arabidopsis thaliana*

169   ELF3 (AtELF3) to search the proteomes of two model monocots *Brachypodium distachyon* and

170   *Setaria viridis* using BLAST (Altschul et al., 1990). Among the top hits, we identified a

171   previously reported ELF3 homolog in *B. distachyon* (*Bradi2g14290.1, BdELF3*) (Calixto et al.,

172   2015; Higgins et al., 2010) and two putative *ELF3* homologous genes *Sevir.5G206400.1*

173   (referred as *SvELF3a*) and *Sevir.3G123200.1* (referred as *SvELF3b*) in *S. viridis.* We used

174   Clustal Omega (http://www.ebi.ac.uk/Tools/msa/clustalo/) to conduct multiple sequence

175   alignments of comparing protein sequences of ELF3 orthologs with that of AtELF3 (Sievers et

176   al., 2011). *BdELF3*, *SvELF3a* and *SvELF3b* encode proteins with similar identity compared to

177   AtELF3 (34.7–36.8%) (**Supplemental Figure S1**). When compared to BdELF3, SvELF3b was

178   74.3% identical while SvELF3a was 57.4% identical (**Supplemental Figure S1**). Therefore, to

179   maximize the diversity of ELF3 sequences used in this study, we cloned full length cDNAs

180   encoding BdELF3 and SvELF3a.

181

182   **Diel Explorer of *S. viridis* circadian data**

183

184   In Arabidopsis, ELF3 cycles under diel and circadian conditions (constant condition after

185   entrainment) with a peak phase in the evening (Covington et al., 2001; Hicks et al., 2001;

186   Nusinow et al., 2011). We queried an available diurnal time course expression dataset for *B.*

187   *distachyon* from the DIURNAL website, and found that *BdELF3* expression cycles under diel

188   conditions (LDHH, 12 h light / 12 h dark cycles with constant temperature), but not under

189   circadian conditions in available data (LDHC-F or LDHH-F, **Supplemental Figure S2**)

190   (Filichkin et al., 2011; Mockler et al., 2007). Also different from *AtELF3,* transcript levels of

191   *BdELF3* accumulate at dawn rather than peak in the evening (**Supplemental Figure S2**) when

192   grown under diel conditions, suggesting different regulations on *ELF3* expression between

193   monocot and dicot plants. Neither diel nor circadian expression data for *S. viridis* was available.

194   Therefore, we generated RNA-seq time-course data to examine *SvELF3* expression as well as the

195   circadian expression of other clock orthologs after both photocycle and thermocycle entrainment.

196   In   addition,   we   developed   the   Diel   Explorer   tool

197   (http://shiny.bioinformatics.danforthcenter.org/diel-explorer/) to query and visualize *S. viridis*

198   circadian-regulated gene expression (**Supplemental Figure S3**). 48,594 *S. viridis* transcripts are

199   represented in the two datasets entrained under either photocycles (LDHH-F) or thermocycles

200   (LLHC-F). With Diel Explorer users can manually enter a list of transcript identifiers, gene

201   ontology (GO) terms, or gene orthologs, plot gene expression, and download data. Alternatively,

202   users can upload files of transcript identifiers or gene orthologs, and/or filter the datasets by

203   entrainment, phase, or significance cut-offs. Data and graphs can be downloaded directly using

204   Diel Explorer. The tool serves as a community resource that can be expanded to include other

205   circadian or diurnal data in the future. The underlying code is available on Github

206   (https://github.com/danforthcenter/diel-explorer).

207

208   Under photoperiod entrainment (LDHH-F), 5,585 of the 48,594 *S. viridis* transcripts are

209   circadian regulated (Bonferroni-adjusted P-Value < 0.001). This proportion of photoperiod-

210   entrained circadian genes (~11.5%) is similar to maize (10.8%), rice (12.6%), and poplar

211   (11.2%) data sets, but much smaller than the approximately 30% reported for *A. thaliana*

212   (Covington et al., 2008; Filichkin et al., 2011; Khan et al., 2010). Under thermocycle

213   entrainment (LLHC-F), 582 of the 48,594 *S. viridis* transcripts are circadian regulated.

214   Therefore, only ~1.2% of *S. viridis* transcripts are circadian cycling under thermocycle

215   entrainment. The ~10-fold reduction in circadian cycling genes between photocycle and

216   thermocycle entrainment (**Supplemental Figure S4**) is interesting considering that there was

217   less than 1% difference in the number of genes with a circadian period between photocycle and

218   thermocycle entrainment in C3 monocot rice (*Oryza japonica*) (Filichkin et al., 2011). The

219   reduction in cycling genes between the two entrainment conditions in *S. viridis* compared to *O.*

220   *japonica* is an indication that circadian regulation could vary greatly among monocots. Also, the

221   difference in number of cycling genes between monocots and dicots may represent a significant

222   reduction of the role of the circadian clock between these lineages.

223

224   In addition to the overall reduction in circadian genes, the phase with the most number of cycling

225   genes was ZT18 after light entrainment (LDHH-F; **Supplemental Figure S4**), but ZT12 with

226   temperature entrainment (LLHC-F; **Supplemental Figure S4**), which is consistent with previous

227   studies that have found significant differences in temperature and light entrainment of the

228   circadian clock (Boikoglou et al., 2011; Michael et al., 2008; Michael et al., 2003). There are 269

229   genes that are considered circadian-regulated and are cycling under both LDHH-F and LLHC-F

230   conditions (Bonferroni Adjusted P-Value < 0.001). The list of 269 genes that overlap between

231   photocycle and thermocycle entrainment includes best matches for Arabidopsis core clock

232   components *TIMING OF CAB EXPRESSION 1* (*TOC1*, *AT5G61380.1*; *Sevir.1G241000.1*),

233   *LATE ELONGATED HYPOCOTYL* (*LHY*, *AT1G01060*; *Sevir.6G053100.1*), and *CCA1*-like gene

234   *REVEILLE1* (*RVE1*, *AT5G17300.1*; *Sevir.1G280700.1*). However, putative *S. viridis* orthologs of

235   *TOC1*, *LHY*, and *RVE1* all have different circadian phases under LDHH entrainment compared

236   to LLHC entrainment (**Figure 1**). In fact, the majority (233/269) of overlapping circadian genes

237   in *S. viridis* have a distinct circadian phase under thermocycle compared to photocycle entrainment

238   (**Supplemental Figure S4**). We also found that putative orthologs of *PSEUDO-RESPONSE*

239   *REGULATOR 7* (*PRR7*,   *AT5G02810*; *Sevir.2G456400.1*; related to *OsPRR73* (Murakami et

240   al., 2003)) and *LUX ARRHYTHMO* (*LUX*, *AT3G46640*; *Sevir.5G474200.1*) cycle significantly

241   under LDHH-F but not LLHC-F conditions (**Figure 1**). Neither *SvELF3a* nor *SvELF3b* cycle

242   under circadian conditions after photo- or thermo-entrainment (**Figure 1**), similar to ELF3

243   orthologs in *B. distachyon* (**Supplemental Figure S2**) (Mockler et al., 2007) and *O. sativa*

244   (Filichkin et al., 2011). This is different from *AtELF3*, which continues to cycle under constant

245   condition after either photo- or thermos-entrainment (**Supplemental Figure S5**) (Mockler et al.,

246   2007). The difference in expression of these putative orthologs between *A. thaliana* and

9

247   monocots *S. viridis*, *B. distachyon*, and *O. sativa*, suggest that the architecture of the circadian

248   clock may have significant differences in response to environmental cues in these two species.

249

250   **BdELF3 and SvELF3 rescue growth and flowering defects in *Arabidopsis elf3* mutant**

251

252   Although the circadian expression pattern of *B. distachyon ELF3* and *S. viridis ELF3* is different

253   from that of *A. thaliana ELF3*, it is still possible that the ELF3 orthologs have conserved

254   biological functions. To test this, we sought to determine if BdELF3 or SvELF3a could

255   complement the major phenotypic defects of the *elf3* mutant in *A. thaliana*, namely hypocotyl

256   elongation, time to flowering, or circadian rhythmicity. To this end, we constitutively expressed

257   *BdELF3*, *SvELF3a* (hereafter referred as *SvELF3*) and *AtELF3* cDNAs by the *35S Cauliflower*

258   *mosaic virus* promoter in the *A. thaliana elf3-2* mutant expressing a *LUCIFERASE* reporter

259   driven by the promoter of *CIRCADIAN CLOCK ASSOCIATED 1* (*CCA1*) (*elf3-2* [*CCA1:LUC*])

260   (Pruneda-Paz et al., 2009). All three ELF3 coding sequences were fused to a C-terminal His$_6$-

261   3xFlag affinity tag (HFC), which enables detection by western blotting and identification of

262   protein-protein interaction by affinity purification and mass spectrometry (AP-MS) (Huang et al.,

263   2016a). After transforming these constructs, we identified and selected two biologically

264   independent transgenic lines with a single insertion of each At/Bd/SvELF3-HFC construct.

265   Western blot analysis using FLAG antibodies detected the expression of all ELF3-HFC fusion

266   proteins (**Supplemental Figure S6**).

267

268   Next, we asked if expressing At/Bd/SvELF3-HFC fusion proteins could rescue the mutation

269   defects caused by *elf3-2*. When plants are grown under light/dark cycles (12 hour light: 12 hour

270   dark), *elf3-2* mutant plants elongate their hypocotyls much more than wild type plants (4.75±0.48

271   mm vs. 1.95±0.27 mm, respectively. ± = standard deviation) (**Figure 2**). The long hypocotyl

272   defect in *elf3-2* was effectively suppressed by expressing either *AtELF3*, or *ELF3* orthologs

273   (*BdELF3 or SvELF3a*) (**Figure 2**). These data show that the monocot *ELF3* orthologs function

274   similarly to *A. thaliana ELF3* in the regulation of hypocotyl elongation in seedlings.

275

10

276   In addition to regulating phenotypes in seedlings, ELF3 also functions in adult plants to suppress
277   the floral transition. Loss-of-function in Arabidopsis *ELF3* results in an early flowering
278   phenotype regardless of day-length (Hicks et al., 2001; Liu et al., 2001; Zagotta et al., 1992). To
279   determine how monocot ELF3 orthologs compared to *A. thaliana* ELF3 in flowering time
280   regulation, we compared flowering responses under long day conditions among wild type, *elf3-2*,
281   and *elf3-2* transgenic lines expressing *AtELF3, BdELF3,* or *SvELF3* (At/Bd/SvELF3-HFC).
282   Constitutive over-expression of *AtELF3* led to a delay in flowering in long days (**Figure 3**) as
283   previously observed (Liu et al., 2001). Similarly, constitutive expression of *BdELF3* or *SvELF3*
284   caused plants to flower significantly later than the *elf3* mutants. These data show that all *ELF3*
285   orthologs can function to repress the rapid transition to flowering of the *elf3* mutation when
286   constitutively expressed in adult plants.

287

288   **BdELF3 and SvELF3 restore the circadian rhythmicity in *Arabidopsis elf3* mutant**

289

290   ELF3 is a key component of the *A. thaliana* circadian clock and is critical for maintaining the
291   periodicity and amplitude of rhythms as shown using the *CCA1* promoter driven luciferase
292   reporter (CCA:LUC) (Covington et al., 2001; Hicks et al., 1996; Nusinow et al., 2011). To
293   determine if *BdELF3* or *SvELF3*a could rescue the arrhythmic phenotype of the *elf3* mutation,
294   we analyzed the rhythms of the *CCA1::LUC* reporter under constant light conditions after diel
295   entrainment (12 hours light: 12 hours dark at constant 22 ˚C). Relative amplitude error (RAE)
296   analysis found that 100% of wild type and nearly all of the three *elf3-2* transgenic lines
297   expressing *AtELF3, BdELF3* (*BdELF3 #3* was 87.5% rhythmic)*,* and *SvELF3* were rhythmic,
298   while only 37.5 % of the *elf3-2* lines had measurable rhythms (RAE < 0.5) (**Supplemental**
299   **Figure S7**). Comparison of average period length found that the *AtELF3* expressing lines
300   completely rescued the period and amplitude defects in the *elf3* mutant (**Figure 4A** and **4D**). The
301   *SvELF3* and *BdELF3* lines also rescued the amplitude defect (**Figure 4B** and **4C**), but their
302   period was longer than wild type (compare 23.21 ± 0.59 hours for wild type to *BdELF3 #2=*
303   27.68 ± 0.86 hours, *BdELF3 #3=* 26.39 ± 1.01 hours, *SvELF3 #2=* 24.47 ± 0.50 hours, *SvELF3*
304   *#3=* 24.32 ± 0.34 hours, and *elf3-2=* 31.27 ± 1.93 hours, ± = standard deviation, **Figure 4D**). In

11

305   summary, these data show that expression of any of the ELF3 orthologs is sufficient to recover

306   the amplitude and restore rhythms of the *CCA1::LUC* reporter.

307

308   **BdELF3 and SvELF3 are integrated into a similar protein-protein interaction network in**

309   ***A. thaliana***

310

311   Despite relatively low sequence conservation at the protein level, the *ELF3* orthologs can

312   complement a wide array of *elf3* phenotypes (**Figures 2** to **4**). As ELF3 functions within the

313   evening complex (EC) in Arabidopsis, which also contains the transcription factor LUX and the

314   DUF-1313 domain containing protein ELF4 (Herrero et al., 2012; Nusinow et al., 2011), we

315   reasoned that the monocot *ELF3* orthologs may also be able to bind to these proteins when

316   expressed in *A. thaliana*. To determine if a composite EC could be formed, we tested if BdELF3

317   or SvELF3a could directly interact with AtLUX or AtELF4 in a yeast two-hybrid assay. Similar

318   to AtELF3 (Nusinow et al., 2011), both BdELF3 and SvELF3a directly interact with both

319   AtELF4 and the C-terminal portion of AtLUX (**Figure 5**). We cannot conclude that whether

320   monocot ELF3 orthologs are also able to interact with the N-terminal AtLUX, since this

321   fragment auto-activated the reporter gene in the yeast two-hybrid assay (**Figure 5**).

322

323   ELF3 functions not only as the scaffold of the EC, but also as a hub protein in a protein-protein

324   interaction network containing multiple key regulators in both the circadian clock and light

325   signaling pathways (Huang et al., 2016a; Huang and Nusinow, 2016b). We hypothesize that

326   BdELF3 and SvELF3 could rescue many of the defects of the *elf3* mutant because both monocot

327   versions were integrated into the same protein-protein interaction network. To test this

328   hypothesis, we used affinity purification and mass spectrometry (AP-MS) to identify the proteins

329   that co-precipitate with monocot ELF3s when expressed in *A. thaliana*. AP-MS on two

330   biological replicates for each sample with the above-mentioned independent insertion lines were

331   included for each ELF3 ortholog. For comparison, the same AP-MS experiment was done with

332   one of the 35S promoter-driven AtELF3-HFC transgenic lines (AtELF3-2). To detect specific

333   co-precipitating proteins, we manually removed commonly identified contaminant proteins from

334   plant affinity purifications and mass spectrometry experiments (Van Leene et al., 2015), and

12

335 proteins identified from a control transgenic line expressing GFP-His$_6$-3xFlag described

336 previously (Huang et al., 2016a) (**Table 1**, the full list of identified proteins can be found in

337 **Supplemental Table S2**).

338

339 We have previously reported proteins that co-precipitated with ELF3 driven from its native

340 promoter using a similar AP-MS methodology (Huang et al., 2016a). When using the 35S

341 promoter driven AtELF3 transgenic line, we were able to generate a curated list of 22 proteins

342 that specifically co-precipitate with AtELF3, including all previously identified proteins, such as

343 all five phytochromes, PHOTOPERIODIC CONTROL OF HYPOCOTYL1 (PCH1) (Huang et

344 al., 2016c), and COP1 (**Table 1**). In addition, we also identified LIGHT-REGULATED WD 2

345 (LWD2) and SPA1-RELATED 4 (SPA4) as now co-precipitating with AtELF3. These additional

346 interactions may be a result of a combination of altered seedling age, expression level of the

347 ELF3 bait, or tissue-specificity of expression due to these purifications are from tissues where

348 the epitope-tagged transgene is constitutively over-expressed. However, since LWD2 is a known

349 component of the circadian clock (Wu et al., 2008) and SPA4 is a known component of the

350 COP1-SPA complex (Zhu et al., 2008), these interactions are likely to be relevant.

351

352 In comparing the list of BdELF3 and SvELF3 co-precipitated proteins with that of AtELF3, we

353 found that neither SvELF3 nor BdELF3 co-precipitated SPA2 and SPA4, components of the

354 COP1-SPA complex. In addition, SvELF3 did not co-precipitate MUT9-LIKE KINASE1, a

355 kinase with roles in chromatin modification and circadian rhythms as AtELF3 did (Huang et al.,

356 2016a; Wang et al., 2015). However, BdELF3 and SvELF3 associated with most of the proteins

357 found in AtELF3 AP-MS (20 out of 22 for BdELF3, 19 out of 22 for SvELF3), in at least one of

358 the replicate purifications from each monocot ortholog AP-MS. Therefore our data suggest that

359 BdELF3 and SvELF3 are integrated into a similar protein-protein interaction network as

360 AtELF3, which likely underlies their ability of broadly complementing *elf3* mutants.

361

362 **DISCUSSION**

363

364   Recent work in diverse plant species has found that the circadian clock plays critical roles in

365   regulating metabolism, growth, photoperiodism, and other agriculturally important traits (Bendix

366   et al., 2015; McClung, 2013; Shor and Green, 2016). While the relevance of the circadian clock

367   to plant fitness is unquestioned, it is unclear if the circadian clock components have conserved

368   function among different plant species. This is particularly true for the majority of clock proteins,

369   whose biological functions are currently poorly understood at the molecular level (Hsu and

370   Harmer, 2014). Also, the divergent modes of growth regulation and photoperiodism between

371   monocots and dicots suggest that the clock evolved to have altered roles in regulating these

372   physiological responses between lineages (Matos et al., 2014; Poire et al., 2010; Song et al.,

373   2014). Here we asked if orthologs of ELF3 from two monocots could complement any of the

374   loss-of-function phenotypes in the model dicot plant *A. thaliana*. In this study we found that

375   ELF3 from either *B. distachyon* or *S. viridis* could complement the hypocotyl elongation, early

376   flowering, and arrhythmic clock phenotype of the *elf3* mutant in *A. thaliana,* despite the

377   variations in protein sequences and evolutionary divergence between monocot and dicot plants.

378   These data suggest that monocot ELF3s can functionally substitute for *A. thaliana* ELF3, albeit

379   with varying efficacy. Since monocot and dicot ELF3 are largely different in the protein

380   sequences, functional conservation of ELF3 orthologs also leads to the next open question of

381   identifying the functional domains within ELF3.

382

383   Previously, comparison of ELF3 homologs has identified at least five conserved regions that may

384   be important for function (**Supplemental Figure S1**) (Liu et al., 2001; Saito et al., 2012; Weller

385   et al., 2012). Our multiple sequence alignments also show that at least two regions of AtELF3,

386   namely the N-terminus (AA 1~49) and one middle region (AA 317~389) share many conserved

387   residues with ELF3 orthologs in grasses (**Supplemental Figure S1**). These regions fall within

388   known fragments that are sufficient for binding to phyB (Liu et al., 2001), COP1 (Yu et al.,

389   2008), or ELF4 (Herrero et al., 2012). Consistent with the hypothesis that these conserved

390   regions are critical for proper ELF3 function, a single amino acid substitution (A362V) within

391   this middle region results in defects of ELF3 nuclear localization and changes in the circadian

392   clock period (Anwer et al., 2014). In addition, our protein-protein interaction study and AP-MS

393   analysis show that both monocot ELF3 can form composite ECs (**Figure 5**) and that all three

14

394　　ELF3 homologs interact with an almost identical set of proteins *in vivo* (**Table 1**), further
395　　suggesting that one or more of the conserved regions may mediate the binding between ELF3
396　　and its known interacting proteins. Furthermore, the similar pool of ELF3 interacting proteins
397　　identified by Bd/SvELF3 AP-MS suggests that the overall conformation of ELF3 ortholog
398　　proteins is conserved and that similar complexes and interactions with ELF3 orthologs may form
399　　in monocot species. However, whether these interactions form *in planta* and have the same effect
400　　on physiology is unclear. For example, *S. viridis* data generated here and public data for *B.*
401　　*distachyon* and *O. sativa*, showed that ELF3 does not cycle under circadian conditions, which
402　　differs from Arabidopsis. Further, different from the fact that the clock plays a key role in
403　　regulating elongation in *A. thaliana* (Nozue et al., 2007)*,* the circadian clock has no influence on
404　　growth in C3 model grass *B. distachyon,* despite robust oscillating expression of putative clock
405　　components (Matos et al., 2014). Similarly, ELF3 from rice *(Oryza sativa)* and soybean
406　　promotes flowering and senescence (Lu et al., 2017; Saito et al., 2012; Sakuraba et al., 2016;
407　　Yang et al., 2013; Zhao et al., 2012), while in *A. thaliana,* ELF3 represses these responses (Liu et
408　　al., 2001; Sakuraba et al., 2014; Zagotta et al., 1992), which suggests significant rewiring of
409　　ELF3 regulated photoperiodic responses of flowering between short-day (rice/soybean) and
410　　long-day (*A. thaliana*) plants. Alternatively, ELF3 may form distinct interactions and complexes
411　　in monocot species that were not identified in our trans-species complementation analysis.
412　　Clearly, further work is required to understand ELF3 function in monocots beyond the studies
413　　presented here.
414

415　　In addition to the molecular characterization of ELF3, our analysis of circadian-regulated genes
416　　in *S. viridis* after photo- and thermo-entrainment found significant differences in the behavior of
417　　the clock when compared to other monocots. Although the number of circadian regulated genes
418　　is comparable to studies done in corn and rice after photo-entrainment (between 10-12%)
419　　(Filichkin et al., 2011; Khan et al., 2010), we found that very few genes (~1%) continue to cycle
420　　after release from temperature entrainment in *S. viridis* (**Supplemental Figure S4**) when
421　　compared to rice (~11%) (Filichkin et al., 2011). This may reflect a fundamental difference in
422　　how the clock interfaces with temperature between these monocot species. Furthermore,
423　　proportions of circadian regulated genes upon photo-entrainment in all three monocot plants

15

424   (**Supplement Figure S4**) (Filichkin et al., 2011; Khan et al., 2010) are much smaller than the

425   approximately 30% reported for *A. thaliana* (Covington et al., 2008), suggesting the divergence

426   of clock functions through evolution or domestication. Further comparisons of circadian

427   responses among monocots or between monocots and dicots will help to determine the molecular

428   underpinning of these differences.

429

430   In summary, we find that BdELF3 and SvELF3 form similar protein complexes *in vivo* as

431   AtELF3, which likely allows for functional complementation of loss-of-function of *elf3* despite

432   relatively low sequence conservation. We also present an online query tool, Diel Explorer that

433   allows for exploration of circadian gene expression in *S. viridis*, which illustrate fundamental

434   differences in clock function among monocots and between monocots and dicots. Collectively,

435   this work is a first step toward functional understanding of the circadian clock in two model

436   monocots, *S. viridis* and *B. distachyon.*

437

438   **MATERIALS AND METHODS**

439

440   **Plant materials and growth conditions**

441

442   For *A. thaliana,* wild type (Columbia-0) and *elf3-2* plants carrying the CCA1::LUC reporter were

443   described previously (Nusinow et al., 2011; Pruneda-Paz et al., 2009). Seeds were surface

444   sterilized and plated on 1/2x Murashige and Skoog (MS) basal salt medium with 0.8% agar + 1%

445   (w/v) sucrose. After 3 days of stratification, plates were placed horizontally in a Percival

446   incubator (Percival Scientific, Perry, IA), supplied with 80 µmol m^{-2} sec^{-1} white light and set to a

447   constant temperature of 22°C. Plants were grown under 12 h light / 12 h dark cycles (12L:12D)

448   for 4 days (for physiological experiments) or for 10 days (for AP-MS) before assays.

449

450   For *S. viridis* circadian expression profiling by RNA-seq, seeds were stratified for 5 days at 4°C

451   before being moved to entrainment conditions. Plants were grown under either LDHH or LLHC

452   (L: light, D: dark, H: hot, C: cold) entrainment condition, and then sampled for RNA-seq in

453   constant light and constant temperature (32°C) conditions (F, for free-running) every 2 hours for

16

454   48 hours. Light intensity was set to 400 µmol m^{-2} sec^{-1} white light. In LDHH-F, stratified *S.*

455   *viridis* seeds were grown for 10 days under 12L:12D and constant temperature (32°C) before

456   sampling in constant light and constant temperature. In LLHC-F, stratified *S. viridis* seeds were

457   grown for 10 days under constant light conditions and cycling temperature conditions 12 h at

458   32°C (subjective day) / 12 h at 22°C (subjective night) before sampling in constant conditions.

459   Two experimental replicates were collected for each entrainment condition.

460

461   **Setaria circadian RNA-seq**

462

463   The second leaf from the top of seventeen *S. viridis* plants was selected for RNA-seq sampling at

464   each time point for each sampling condition. Five replicate samples were pooled after being

465   ground in liquid nitrogen and resuspended in lithium chloride lysis binding buffer (Wang et al.,

466   2011a). RNA-seq libraries from leaf samples were constructed according to the previous

467   literature (Wang et al., 2011a) with one major modification. Rather than extracting RNA then

468   mRNA from ground leaf samples (Wang et al., 2011a), mRNA was extracted directly from

469   frozen ground leaf samples similar to the method described in (Kumar et al., 2012), except that

470   two additional rounds of wash, binding, and elution steps after treatment with EDTA were

471   necessary to remove rRNA from samples. mRNA quantity was assessed using a Qubit with a

472   Qubit RNA HS Kit and mRNA quality was assessed using a Bioanalyzer and Plant RNA PiCO

473   chip. 96 library samples were multiplexed 12 per lane, for a total of 8 lanes of Illumina Hiseq

474   2000 sequencing. Paired end 101 bp Sequencing was done at MOgene (St. Louis, MO). Raw

475   data and processed data can be found on NCBI's Gene Expression Omnibus (GEO; (Barrett et

476   al., 2013; Edgar et al., 2002)) and are accessible with identification number GSE97739

477   (https://www.ncbi.nlm.nih.gov/geo/query/acc.cgi?acc=GSE97739).

478

479   RNA-seq data was trimmed with BBTools (v36.20) using parameters: ktrim=r k=23 mink=11

480   hdist=1 tpe tbo ktrim=l k=23 mink=11 hdist=1 tpe tbo qtrim=rl trimq=20 minlen=20 (Bushnell,

481   2016). Any parameters not specified were run as default. Before trimming we had 1,814,939,650

482   reads with a mean of 18,905,621 reads per sample and a standard deviation of 2,875,187. After

483   trimming, we have 1,646,019,593 reads with a mean of 17,146,037 reads per sample and a

17

484   standard deviation of 2,411,061. Kallisto (v 0.42.4; (Bray et al., 2016)) was used to index the

485   transcripts with the default parameters and the *S. viridis* transcripts fasta file (Sviridis_311_v1.1)

486   from Phytozome (Goodstein et al., 2012). The reads were quantified with parameters:-t 40 -b

487   100. Any parameters not specified were run as default. Kallisto output was formatted for

488   compatibility with JTKCycle (v3.1; (Hughes et al., 2010)) and circadian cycles were detected.

489   To query the *S. viridis* expression data we developed Diel Explorer. The tool can be found at

490   http://shiny.bioinformatics.danforthcenter.org/diel-explorer/. Underlying code for Diel Explorer

491   is available on Github (https://github.com/danforthcenter/diel-explorer).

492

493   **Plasmid constructs and generation of transgenic plants**

494

495   Coding sequences (without the stop codon) of *AtELF3* (*AT2G25930*) and *SvELF3a*

496   (*Sevir.5G206400.1*) were cloned into the pENTR/D-TOPO vector (ThermoFisher Scientific,

497   Waltham, MA), verified by sequencing and were recombined into the pB7HFC vector (Huang et

498   al., 2016a) using LR Clonease (ThermoFisher Scientific, Waltham, MA). Coding sequence of

499   BdELF3 (*Bradi2g14290.1*) was submitted to the U.S. Department of Energy Joint Genome

500   Institute (DOE-JGI), synthesized by the DNA Synthesis Science group, and cloned into the

501   pENTR/D-TOPO vector. Sequence validated clones were then recombined into pB7HFC as

502   described above. The pB7HFC-At/Bd/SvELF3 constructs were then transformed into *elf3-2*

503   [*CCA1::LUC*] plants by the floral dip method (Zhang et al., 2006). Homozygous transgenic

504   plants were validated by testing luciferase bioluminescence, drug resistance, and by PCR-based

505   genotyping. All primers used in this paper were listed in **Supplemental Table S1**.

506

507   **Hypocotyl and flowering time measurement**

508

509   20 seedlings of each genotype were arrayed and photographed with a ruler for measuring

510   hypocotyl length using the ImageJ software (NIH) (Schneider et al., 2012). The procedure was

511   repeated three times. For measuring flowering time, 12 plants of each genotype were placed in a

512   random order and were grown under the long day condition (light : dark = 16 : 8 hours). The

513   seedlings were then observed every day at 12:00 PM; the date on which each seedling began

514   flowering, indicated by the growth of a ~1 cm inflorescence stem, was recorded along with the

515   number of rosette leaves produced up to that date. ANOVA analysis with Bonferroni correction

516   was measured using GraphPad Prism version 6.00 (GraphPad Software, La Jolla California

517   USA, www.graphpad.com).

518

519   **Circadian assays in *A. thaliana***

520

521   Seedlings were transferred to fresh 1/2x MS plates after 5 days of entrainment under the

522   12L:12D condition and sprayed with sterile 5 mM luciferin (Gold Biotechnology, St. Louis, MO)

523   prepared in 0.1% (v/v) Triton X-100 solution. Sprayed seedlings were then imaged in constant

524   light (70 µmol m^{-2} sec^{-1}, wavelengths 400, 430, 450, 530, 630, and 660 set at intensity 350

525   (Heliospectra LED lights, Göteborg, Sweden)). Bioluminescence was recorded after a 120-180s

526   delay to diminish delayed fluorescence (Gould et al., 2009) over 5 days using an ultra-cooled

527   CCD camera (Pixis 1024B, Princeton Instruments) driven by Micro-Manager software (Edelstein

528   et al., 2010; Edelstein et al., 2014). The images were processed in stacks by Metamorph software

529   (Molecular Devices, Sunnyvale, CA), and rhythms determined by fast Fourier transformed non-

530   linear least squares (FFT-NLLS) (Plautz et al., 1997) after background subtraction using the

531   interface provided by the Biological Rhythms Analysis Software System 3.0 (BRASS) available

532   at http://www.amillar.org.

533

534   **Yeast two-hybrid analysis**

535

536   Yeast two-hybrid assays were carried out as previously described (Huang et al., 2016a). In brief,

537   the DNA binding domain (DBD) or activating domain (AD)-fused constructs were transformed

538   using the Li-Ac transformation protocol (Clontech) into *Saccharomyces cerevisiae* strain Y187

539   (MATα) and the AH109 (MATa), respectively. Two strains of yeast were then mated to generate

540   diploid with both DBD and AD constructs. Protein-protein interaction was tested in diploid yeast

541   by replica plating on CSM –Leu –Trp –His media supplemented with extra Adenine (30mg/L

542   final concentration) and 2mM 3-Amino-1,2,4-triazole (3AT). Pictures were taken after 4-day

543   incubation at 30 ˚C. All primers used for cloning plasmid constructs were listed in
544   **Supplemental Table S1**.

545

546   **Protein extraction and western blotting**

547

548   Protein extracts were made from 10-day-old seedlings as previously described (Huang et al.,
549   2016a) and loaded 50 μg to run 10% SDS-PAGE. For western blots, all of the following primary
550   and secondary antibodies were diluted into PBS + 0.1% Tween and incubated at room
551   temperature for 1 hour: anti-FLAG®M2-HRP (Sigma, A8592, diluted at 1:10,000) and anti-
552   Rpt5-rabbit (ENZO Life Science, BML-PW8245-0025, diluted at 1:5000) and anti-Rabbit-HRP
553   secondary antibodies (Sigma, A0545, diluted at 1:10,000).

554

555   **Affinity purification and mass spectrometry**

556

557   Protein extraction methods and protocols for AP-MS were described previously (Huang et al.,
558   2016a; Huang et al., 2016b; Huang and Nusinow, 2016a; Huang et al., 2016c)}. In brief,
559   transgenic seedlings carrying the At/Bd/SvELF3-HFC constructs were grown under 12L:12D
560   conditions for 10 days and were harvested at dusk (ZT12). 5 grams of seedlings were needed per
561   replicate to make protein extracts, which underwent tandem affinity purification utilizing the
562   FLAG and His epitopes of the fusion protein. Purified samples were reduced, alkylated and
563   digested by trypsin. The tryptic peptides were then injected to an LTQ-Orbitrap Velos Pro
564   (ThermoFisher Scientific, Waltham, MA) coupled with a U3000 RSLCnano HPLC
565   (ThermoFisher Scientific, Waltham, MA) with settings described previously (Huang et al.,
566   2016a).

567

568   **AP-MS data analysis**

569

570   Data analysis was done as previously described (Huang et al., 2016a). The databases searched
571   were TAIR10 database (20101214, 35,386 entries) and the cRAP database
572   (http://www.thegpm.org/cRAP/). Peptide identifications were accepted if they could be

573 established at greater than 95.0% probability and the Scaffold Local FDR was <1%. Protein

574 identifications were accepted if they could be established at greater than 99.0% probability as

575 assigned by the Protein Prophet algorithm (Keller et al., 2002; Nesvizhskii et al., 2003). A full

576 list of all identified proteins (reporting total/exclusive unique peptide count and percent

577 coverage) can be found in **Supplemental Table S2**. The mass spectrometry proteomics data

578 have been deposited to the ProteomeXchange Consortium (Vizcaino et al., 2014) via the PRIDE

579 partner repository with the dataset identifier PXD006352 and 10.6019/PXD006352.

580

581

582 **Supplemental Data**

583 **Supplemental Table S1.** List of all primers used.

584 **Supplemental Table S2.** A full list of At/Bd/SvELF3 associated proteins identified from AP-

585 MS.

586 **Supplemental Figure S1.** Multiple sequence alignments of ELF3 orthologs

587 **Supplemental Figure S2.** Diel and circadian expression of *BdELF3* from the DIURNAL

588 database.

589 **Supplemental Figure S3.** Example of the Diel Explorer interface.

590 **Supplemental Figure S4.** Summary of circadian regulated genes in *S. viridis.*

591 **Supplemental Figure S5.** Circadian expression of selected *A. thaliana* clock genes from the

592 DIURNAL database.

593 **Supplemental Figure S6.** Anti-FLAG western of ELF3 transgenic lines used for

594 complementation analysis.

595 **Supplemental Figure S7.** Relative Amplitude Error vs period plots of transgenic *elf3-2* plants

596 expressing At/Bd/SvELF3.

597

Table 1. Proteins co-purified with ELF3 orthologs from AP-MS

AGI number	Protein Name	Molecular Weight	Exclusive Unique Peptide Count/Percent Coverage [a]									
			AtELF3		SvELF3 #2		SvELF3 #3		BdELF3 #2		BdELF3 #3	
			rep1	rep2	rep1	rep2	rep1	rep2	rep1	rep2	rep1	rep2
n/a	AtELF3-HFC	84 kDa	20/36%	19/31%	—	—	—	—	—	—	—	—
n/a	SvELF3-HFC	87 kDa	—	—	19/40%	29/48%	22/42%	33/54%	—	—	—	—
n/a	BdELF3-HFC	86 kDa	—	—	—	—	—	—	25/42%	26/43%	21/35%	19/33%
AT2G18790	phyB	129 kDa	23/37%	24/37%	31/54%	28/42%	32/50%	30/45%	22/34%	22/33%	24/40%	24/37%
AT5G35840	phyC	124 kDa	22/29%	23/29%	27/37%	32/39%	27/37%	33/42%	20/24%	18/22%	19/23%	22/27%
AT5G43630	TZP	91 kDa	14/21%	12/17%	13/23%	20/33%	13/22%	24/36%	12/18%	13/19%	14/20%	14/22%
AT4G18130	phyE	123 kDa	11/16%	19/27%	12/18%	18/23%	11/19%	17/24%	6/7%	10/14%	14/19%	13/18%
AT2G16365.2	PCH1[b]	51 kDa	9/25%	9/25%	9/30%	14/43%	11/36%	16/49%	9/26%	9/28%	11/32%	11/32%
AT2G46340	SPA1	115 kDa	8/14%	7/9%	2/2%	4/8%	2/3%	4/9%	—	—	6/8%	5/6%
AT3G42170[c]	DAYSLEEPER	79 kDa	8/19%	5/11%	—	7/16%	—	12/27%	3/7%	4/8%	2/4%	—
AT2G32950	COP1	76 kDa	8/16%	9/17%	6/17%	4/8%	3/6%	5/12%	1/2%	2/4%	6/11%	4/8%
AT3G22380	TIC	165 kDa	5/5%	5/5%	4/4%	12/12%	3/3%	15/15%	4/4%	3/3%	1/1%	1/1%
AT4G11110	SPA2	115 kDa	5/11%	6/12%	—	—	—	—	—	—	—	—
AT2G40080	ELF4	12 kDa	4/50%	4/50%	3/42%	5/68%	4/60%	4/60%	4/50%	4/50%	5/68%	5/68%
AT1G09340[c]	CRB	43 kDa	4/16%	3/12%	1/4%	1/4%	1/4%	4/18%	1/4%	1/4%	—	—
AT3G13670	MLK4	79 kDa	3/10%	3/13%	—	—	—	1/2%	6/21%	3/10%	3/11%	5/13%
AT5G61380	TOC1	69 kDa	2/4%	2/4%	2/5%	—	3/7%	—	—	—	1/2%	1/2%
AT1G53090	SPA4	89 kDa	2/6%	5/14%	—	—	—	—	—	—	—	—
AT5G18190	MLK1	77 kDa	2/12%	2/11%	—	—	—	—	2/14%	2/14%	2/11%	2/11%
AT3G26640	LWD2	39 kDa	2/21%	1/21%	—	1/16%	—	2/22%	3/27%	1/16%	—	—
AT1G12910	LWD1	39 kDa	2/21%	3/30%	2/21%	4/31%	1/17%	2/21%	2/22%	2/19%	0/11%	0/11%
AT4G16250	phyD	129 kDa	1/10%	1/11%	2/12%	1/12%	3/15%	2/12%	2/11%	1/10%	2/14%	2/12%
AT1G09570	phyA	125 kDa	1/1%	1/1%	7/11%	5/5%	7/11%	2/2%	—	2/2%	6/7%	3/4%

Gene	Name	Size										
AT2G25760	MLK3	76 kDa	1/5%	1/6%	—	1/4%	—	1/4%	3/13%	2/9%	2/9%	2/9%
AT3G03940	MLK2	78 kDa	1/8%	1/8%	—	1/7%	—	0/2%	3/20%	2/13%	3/13%	1/9%
AT3G46640	LUX	35 kDa	1/3%	1/3%	0/10%	3/19%	0/10%	3/23%	1/3%	1/3%	1/3%	2/11%
AT1G17455	ELF4-L4	13 kDa	—	—	—	—	—	—	1/23%	1/23%	—	—
AT1G72630	ELF4-L2	13 kDa	—	1/11%	—	1/13%	—	—	1/22%	1/22%	1/22%	1/11%

Proteins co-purified with ELF3 orthologs (AtELF3, SvELF3 and BdELF3, with C-terminal His6-3xFLAG tag) were identified from affinity purification coupled with mass spectrometry (AP-MS) analyses using 12L:12D grown, 10-day-old transgenic plants (in *elf3-2 null* mutant backgrounds) harvested at ZT12.

[a] All listed proteins match 99% protein threshold, minimum number peptides of 2 and peptide threshold as 95%. Proteins not matching the criteria were marked with "—".

[b] Percent coverage for PCH1 is calculated using protein encoded by *At2g16365.2*

[c] These proteins have been noted as frequently identified proteins in AP-MS experiments (see Van Leene, 2015).

2

598 **FIGURE LEGENDS**

599

600 **Figure 1.** Circadian expression profiles of putative *S. viridis* clock components from Diel

601 Explorer using time-course RNA-seq data. *S. viridis* plants were entrained by either photocycle

602 (LDHH) or thermocycle (LLHC), followed by being sampled every 2 hours for 48 hours under

603 constant temperature and light conditions (Free-Running; F) to generate time-course RNA-seq

604 data. Mean values of Transcripts per Kilobase Million (TPM) from two experimental replicates

605 for each timepoints per gene were plotted.

606

607 **Figure 2.** ELF3 orthologs suppress hypocotyl elongation defects in *elf3-2*. The hypocotyls of 20

608 seedlings of wild type, *elf3-2* mutant, AtELF3 *elf3-2*, BdELF3 *elf3-2*, and SvELF3 *elf3-2* (two

609 independent transgenic lines for each ELF3 ortholog) were measured at 4 days after germination

610 under 12-hour light :12-hour dark growth conditions at 22 ˚C. Upper panel shows representative

611 seedlings of each genotype, with scale bar equal to 5 mm. Mean and 95% confidence intervals

612 are plotted as crosshairs. This experiment was repeated three times with similar results. ANOVA

613 analysis with Bonferroni correction was used to generate adjusted P values, * < 0.05, ** < 0.01,

614 **** < 0.0001**.**

615

616 **Figure 3.** ELF3 orthologs suppress time to flowering of *elf3-2*. 12 wild type, *elf3-2* mutant,

617 AtELF3 *elf3-2*, BdELF3 *elf3-2*, and SvELF3 *elf3-2* seedlings from two independent

618 transformations were measured for days (**A**) and number of rosette leaves (**B**) at flowering (1 cm

619 inflorescence). Mean and 95% confidence intervals are plotted as crosshairs. This experiment

620 was repeated twice with similar results. ANOVA analysis with Bonferroni correction was used to

621 generate adjusted P values, ** < 0.01, *** < 0.001, **** < 0.0001, of measurements when

622 compared to the *elf3-2* mutant line.

623

624 **Figure 4.** ELF3 orthologs can recover *CCA1::LUC* rhythms and amplitude in *elf3-2* mutants. 8

625 seedlings of wild type, *elf3-2* mutant, AtELF3 *elf3-2* (**A**), BdELF3 *elf3-2* (**B**), and SvELF3 *elf3-2*

626 (**C**) from two independent transformations were imaged for bioluminescence under constant light

627 after entrainment in 12-hour light :12-hour dark growth conditions at 22 ˚C. Each plot shows

1

628   average bioluminescence of all seedlings along with 95% confidence interval (error bars). This

629   experiment was repeated four times with similar results. Note that wild type and *elf3-2* mutant

630   data was plotted on all graphs for comparison. **(D)** Periods of seedlings. Only periods with a

631   Relative Amplitude Error below 0.5 (see **Supplemental Figure S7**) were plotted. Mean and 95%

632   confidence intervals are plotted as crosshairs. ANOVA analysis with Bonferroni correction was

633   used to generate adjusted P values, $* < 0.05$, $** < 0.01$, $*** < 0.001$, $**** < 0.0001$, of

634   measurements when compared to the wild type.

635

636   **Figure 5.** Both BdELF3 and SvELF3 can directly bind to AtELF4 and AtLUX. Yeast two-hybrid

637   analysis of testing if either BdELF3 **(A)** or SvELF3 **(B)** can directly interact with either AtELF4,

638   the N-terminal half of AtLUX (AtLUX-N, a.a. 1-143) or the C-terminal half of AtLUX (AtLUX-

639   C, a.a. 144-324). –LW tests for the presence of both bait (DBD) and pray (AD) vectors, while the

640   –LWH + 3AT tests for interaction. Vector alone serves as interaction control. This experiment

641   was repeated twice with similar results.

642

643

644

645   **REFERENCES**

646

647   Altschul, S.F., Gish, W., Miller, W., Myers, E.W., and Lipman, D.J. (1990). Basic local alignment
648   search tool. J Mol Biol *215*, 403-410.
649   Anwer, M.U., Boikoglou, E., Herrero, E., Hallstein, M., Davis, A.M., Velikkakam James, G., Nagy,
650   F., and Davis, S.J. (2014). Natural variation reveals that intracellular distribution of ELF3 protein
651   is associated with function in the circadian clock. Elife *3*.
652   Barrett, T., Wilhite, S.E., Ledoux, P., Evangelista, C., Kim, I.F., Tomashevsky, M., Marshall, K.A.,
653   Phillippy, K.H., Sherman, P.M., Holko, M.*, et al.* (2013). NCBI GEO: archive for functional
654   genomics data sets--update. Nucleic Acids Res *41*, D991-995.
655   Bell-Pedersen, D., Cassone, V.M., Earnest, D.J., Golden, S.S., Hardin, P.E., Thomas, T.L., and
656   Zoran, M.J. (2005). Circadian rhythms from multiple oscillators: lessons from diverse organisms.
657   Nat Rev Genet *6*, 544-556.
658   Bendix, C., Marshall, C.M., and Harmon, F.G. (2015). Circadian Clock Genes Universally Control
659   Key Agricultural Traits. Mol Plant *8*, 1135-1152.

660   Bennetzen, J.L., Schmutz, J., Wang, H., Percifield, R., Hawkins, J., Pontaroli, A.C., Estep, M., Feng,
661   L., Vaughn, J.N., Grimwood, J., *et al.* (2012). Reference genome sequence of the model plant
662   Setaria. Nat Biotechnol *30*, 555-561.
663   Boikoglou, E., Ma, Z., von Korff, M., Davis, A.M., Nagy, F., and Davis, S.J. (2011). Environmental
664   memory from a circadian oscillator: the Arabidopsis thaliana clock differentially integrates
665   perception of photic vs. thermal entrainment. Genetics *189*, 655-664.
666   Bray, N.L., Pimentel, H., Melsted, P., and Pachter, L. (2016). Near-optimal probabilistic RNA-seq
667   quantification. Nat Biotech *34*, 525-527.
668   Brutnell, T.P., Wang, L., Swartwood, K., Goldschmidt, A., Jackson, D., Zhu, X.G., Kellogg, E., and
669   Van Eck, J. (2010). Setaria viridis: a model for C4 photosynthesis. Plant Cell *22*, 2537-2544.
670   Bushnell, B. (2016). BBMap short read aligner. University of California, Berkeley, California URL
671   http://sourceforge net/projects/bbmap.
672   Calixto, C.P., Waugh, R., and Brown, J.W. (2015). Evolutionary relationships among barley and
673   Arabidopsis core circadian clock and clock-associated genes. J Mol Evol *80*, 108-119.
674   Covington, M.F., Maloof, J.N., Straume, M., Kay, S.A., and Harmer, S.L. (2008). Global
675   transcriptome analysis reveals circadian regulation of key pathways in plant growth and
676   development. Genome Biol *9*, R130.
677   Covington, M.F., Panda, S., Liu, X.L., Strayer, C.A., Wagner, D.R., and Kay, S.A. (2001). ELF3
678   modulates resetting of the circadian clock in Arabidopsis. Plant Cell *13*, 1305-1315.
679   Dixon, L.E., Knox, K., Kozma-Bognar, L., Southern, M.M., Pokhilko, A., and Millar, A.J. (2011).
680   Temporal repression of core circadian genes is mediated through EARLY FLOWERING 3 in
681   Arabidopsis. Curr Biol *21*, 120-125.
682   Dodd, A.N., Salathia, N., Hall, A., Kevei, E., Toth, R., Nagy, F., Hibberd, J.M., Millar, A.J., and
683   Webb, A.A. (2005). Plant circadian clocks increase photosynthesis, growth, survival, and
684   competitive advantage. Science *309*, 630-633.
685   Doherty, C.J., and Kay, S.A. (2010). Circadian control of global gene expression patterns. Annu
686   Rev Genet *44*, 419-444.
687   Doyle, M.R., Davis, S.J., Bastow, R.M., McWatters, H.G., Kozma-Bognar, L., Nagy, F., Millar, A.J.,
688   and Amasino, R.M. (2002). The ELF4 gene controls circadian rhythms and flowering time in
689   Arabidopsis thaliana. Nature *419*, 74-77.
690   Edelstein, A., Amodaj, N., Hoover, K., Vale, R., and Stuurman, N. (2010). Computer control of
691   microscopes using microManager. Curr Protoc Mol Biol *Chapter 14*, Unit14 20.
692   Edelstein, A.D., Tsuchida, M.A., Amodaj, N., Pinkard, H., Vale, R.D., and Stuurman, N. (2014).
693   Advanced methods of microscope control using muManager software. J Biol Methods *1*.
694   Edgar, R., Domrachev, M., and Lash, A.E. (2002). Gene Expression Omnibus: NCBI gene
695   expression and hybridization array data repository. Nucleic Acids Res *30*, 207-210.
696   Edgar, R.S., Green, E.W., Zhao, Y., van Ooijen, G., Olmedo, M., Qin, X., Xu, Y., Pan, M.,
697   Valekunja, U.K., Feeney, K.A., *et al.* (2012). Peroxiredoxins are conserved markers of circadian
698   rhythms. Nature *485*, 459-464.
699   Faure, S., Turner, A.S., Gruszka, D., Christodoulou, V., Davis, S.J., von Korff, M., and Laurie, D.A.
700   (2012). Mutation at the circadian clock gene EARLY MATURITY 8 adapts domesticated barley
701   (Hordeum vulgare) to short growing seasons. Proc Natl Acad Sci U S A *109*, 8328-8333.

702   Filichkin, S.A., Breton, G., Priest, H.D., Dharmawardhana, P., Jaiswal, P., Fox, S.E., Michael, T.P.,
703   Chory, J., Kay, S.A., and Mockler, T.C. (2011). Global profiling of rice and poplar transcriptomes
704   highlights key conserved circadian-controlled pathways and cis-regulatory modules. PLoS One
705   *6*, e16907.
706   Goodstein, D.M., Shu, S., Howson, R., Neupane, R., Hayes, R.D., Fazo, J., Mitros, T., Dirks, W.,
707   Hellsten, U., Putnam, N., *et al.* (2012). Phytozome: a comparative platform for green plant
708   genomics. Nucleic Acids Res *40*, D1178-1186.
709   Gould, P.D., Diaz, P., Hogben, C., Kusakina, J., Salem, R., Hartwell, J., and Hall, A. (2009). Delayed
710   fluorescence as a universal tool for the measurement of circadian rhythms in higher plants.
711   Plant J *58*, 893-901.
712   Graf, A., Schlereth, A., Stitt, M., and Smith, A.M. (2010). Circadian control of carbohydrate
713   availability for growth in Arabidopsis plants at night. Proc Natl Acad Sci U S A *107*, 9458-9463.
714   Greenham, K., and McClung, C.R. (2015). Integrating circadian dynamics with physiological
715   processes in plants. Nat Rev Genet *16*, 598-610.
716   Harmer, S.L. (2009). The circadian system in higher plants. Annu Rev Plant Biol *60*, 357-377.
717   Harmer, S.L., Hogenesch, J.B., Straume, M., Chang, H.S., Han, B., Zhu, T., Wang, X., Kreps, J.A.,
718   and Kay, S.A. (2000). Orchestrated transcription of key pathways in Arabidopsis by the circadian
719   clock. Science *290*, 2110-2113.
720   Hazen, S.P., Schultz, T.F., Pruneda-Paz, J.L., Borevitz, J.O., Ecker, J.R., and Kay, S.A. (2005). LUX
721   ARRHYTHMO encodes a Myb domain protein essential for circadian rhythms. Proc Natl Acad Sci
722   U S A *102*, 10387-10392.
723   Helfer, A., Nusinow, D.A., Chow, B.Y., Gehrke, A.R., Bulyk, M.L., and Kay, S.A. (2011). LUX
724   ARRHYTHMO encodes a nighttime repressor of circadian gene expression in the Arabidopsis
725   core clock. Curr Biol *21*, 126-133.
726   Herrero, E., Kolmos, E., Bujdoso, N., Yuan, Y., Wang, M., Berns, M.C., Uhlworm, H., Coupland,
727   G., Saini, R., Jaskolski, M., *et al.* (2012). EARLY FLOWERING4 recruitment of EARLY FLOWERING3
728   in the nucleus sustains the Arabidopsis circadian clock. Plant Cell *24*, 428-443.
729   Hicks, K.A., Albertson, T.M., and Wagner, D.R. (2001). EARLY FLOWERING3 encodes a novel
730   protein that regulates circadian clock function and flowering in Arabidopsis. Plant Cell *13*, 1281-
731   1292.
732   Hicks, K.A., Millar, A.J., Carre, I.A., Somers, D.E., Straume, M., Meeks-Wagner, D.R., and Kay,
733   S.A. (1996). Conditional circadian dysfunction of the Arabidopsis early-flowering 3 mutant.
734   Science *274*, 790-792.
735   Higgins, J.A., Bailey, P.C., and Laurie, D.A. (2010). Comparative genomics of flowering time
736   pathways using Brachypodium distachyon as a model for the temperate grasses. PLoS One *5*,
737   e10065.
738   Hsu, P.Y., and Harmer, S.L. (2014). Wheels within wheels: the plant circadian system. Trends in
739   plant science *19*, 240-249.
740   Huang, H., Alvarez, S., Bindbeutel, R., Shen, Z., Naldrett, M.J., Evans, B.S., Briggs, S.P., Hicks,
741   L.M., Kay, S.A., and Nusinow, D.A. (2016a). Identification of Evening Complex Associated
742   Proteins in Arabidopsis by Affinity Purification and Mass Spectrometry. Mol Cell Proteomics *15*,
743   201-217.

744   Huang, H., Alvarez, S., and Nusinow, D.A. (2016b). Data on the identification of protein
745   interactors with the Evening Complex and PCH1 in Arabidopsis using tandem affinity
746   purification and mass spectrometry (TAP-MS). Data Brief *8*, 56-60.
747   Huang, H., and Nusinow, D. (2016a). Tandem Purification of His6-3x FLAG Tagged Proteins for
748   Mass Spectrometry from Arabidopsis. Bio-Protocol *6*.
749   Huang, H., and Nusinow, D.A. (2016b). Into the Evening: Complex Interactions in the
750   Arabidopsis Circadian Clock. Trends Genet *32*, 674-686.
751   Huang, H., Yoo, C.Y., Bindbeutel, R., Goldsworthy, J., Tielking, A., Alvarez, S., Naldrett, M.J.,
752   Evans, B.S., Chen, M., and Nusinow, D.A. (2016c). PCH1 integrates circadian and light-signaling
753   pathways to control photoperiod-responsive growth in Arabidopsis. eLife *5*, e13292.
754   Hughes, M.E., Hogenesch, J.B., and Kornacker, K. (2010). JTK_CYCLE: an efficient nonparametric
755   algorithm for detecting rhythmic components in genome-scale data sets. J Biol Rhythms *25*,
756   372-380.
757   Keller, A., Nesvizhskii, A.I., Kolker, E., and Aebersold, R. (2002). Empirical Statistical Model To
758   Estimate the Accuracy of Peptide Identifications Made by MS/MS and Database Search.
759   Analytical Chemistry *74*, 5383-5392.
760   Khan, S., Rowe, S.C., and Harmon, F.G. (2010). Coordination of the maize transcriptome by a
761   conserved circadian clock. BMC Plant Biol *10*, 126.
762   Khanna, R., Kikis, E.A., and Quail, P.H. (2003). EARLY FLOWERING 4 functions in phytochrome B-
763   regulated seedling de-etiolation. Plant Physiol *133*, 1530-1538.
764   Kim, W.Y., Hicks, K.A., and Somers, D.E. (2005). Independent roles for EARLY FLOWERING 3 and
765   ZEITLUPE in the control of circadian timing, hypocotyl length, and flowering time. Plant Physiol
766   *139*, 1557-1569.
767   Kolmos, E., Herrero, E., Bujdoso, N., Millar, A.J., Toth, R., Gyula, P., Nagy, F., and Davis, S.J.
768   (2011). A reduced-function allele reveals that EARLY FLOWERING3 repressive action on the
769   circadian clock is modulated by phytochrome signals in Arabidopsis. Plant Cell *23*, 3230-3246.
770   Kumar, R., Ichihashi, Y., Kimura, S., Chitwood, D.H., Headland, L.R., Peng, J., Maloof, J.N., and
771   Sinha, N.R. (2012). A High-Throughput Method for Illumina RNA-Seq Library Preparation. Front
772   Plant Sci *3*, 202.
773   Liu, X.L., Covington, M.F., Fankhauser, C., Chory, J., and Wagner, D.R. (2001). ELF3 encodes a
774   circadian clock-regulated nuclear protein that functions in an Arabidopsis PHYB signal
775   transduction pathway. Plant Cell *13*, 1293-1304.
776   Lou, P., Wu, J., Cheng, F., Cressman, L.G., Wang, X., and McClung, C.R. (2012). Preferential
777   retention of circadian clock genes during diploidization following whole genome triplication in
778   Brassica rapa. Plant Cell *24*, 2415-2426.
779   Lu, S., Zhao, X., Hu, Y., Liu, S., Nan, H., Li, X., Fang, C., Cao, D., Shi, X., Kong, L., *et al.* (2017).
780   Natural variation at the soybean J locus improves adaptation to the tropics and enhances yield.
781   Nat Genet.
782   Matos, D.A., Cole, B.J., Whitney, I.P., MacKinnon, K.J., Kay, S.A., and Hazen, S.P. (2014). Daily
783   changes in temperature, not the circadian clock, regulate growth rate in Brachypodium
784   distachyon. PLoS One *9*, e100072.

785   Matsubara, K., Ogiso-Tanaka, E., Hori, K., Ebana, K., Ando, T., and Yano, M. (2012). Natural
786   variation in Hd17, a homolog of Arabidopsis ELF3 that is involved in rice photoperiodic
787   flowering. Plant Cell Physiol *53*, 709-716.
788   McClung, C.R. (2013). Beyond Arabidopsis: the circadian clock in non-model plant species.
789   Semin Cell Dev Biol *24*, 430-436.
790   Michael, T.P., Mockler, T.C., Breton, G., McEntee, C., and Byer, A. (2008). Network discovery
791   pipeline elucidates conserved time-of-day-specific cis-regulatory modules. PLoS genetics.
792   Michael, T.P., Salome, P.A., and McClung, C.R. (2003). Two Arabidopsis circadian oscillators can
793   be distinguished by differential temperature sensitivity. Proc Natl Acad Sci U S A *100*, 6878-
794   6883.
795   Mizuno, T., Nomoto, Y., Oka, H., Kitayama, M., Takeuchi, A., Tsubouchi, M., and Yamashino, T.
796   (2014). Ambient temperature signal feeds into the circadian clock transcriptional circuitry
797   through the EC night-time repressor in Arabidopsis thaliana. Plant Cell Physiol *55*, 958-976.
798   Mockler, T.C., Michael, T.P., Priest, H.D., Shen, R., Sullivan, C.M., Givan, S.A., McEntee, C., Kay,
799   S.A., and Chory, J. (2007). The DIURNAL project: DIURNAL and circadian expression profiling,
800   model-based pattern matching, and promoter analysis. Cold Spring Harb Symp Quant Biol *72*,
801   353-363.
802   Murakami, M., Ashikari, M., Miura, K., Yamashino, T., and Mizuno, T. (2003). The Evolutionarily
803   Conserved OsPRR Quintet: Rice Pseudo-Response Regulators Implicated in Circadian Rhythm.
804   Plant and Cell Physiology *44*, 1229-1236.
805   Nagel, D.H., and Kay, S.A. (2012). Complexity in the wiring and regulation of plant circadian
806   networks. Curr Biol *22*, R648-657.
807   Nesvizhskii, A.I., Keller, A., Kolker, E., and Aebersold, R. (2003). A Statistical Model for
808   Identifying Proteins by Tandem Mass Spectrometry. Analytical Chemistry *75*, 4646-4658.
809   Nozue, K., Covington, M.F., Duek, P.D., Lorrain, S., Fankhauser, C., Harmer, S.L., and Maloof, J.N.
810   (2007). Rhythmic growth explained by coincidence between internal and external cues. Nature
811   *448*, 358-361.
812   Nusinow, D.A., Helfer, A., Hamilton, E.E., King, J.J., Imaizumi, T., Schultz, T.F., Farre, E.M., and
813   Kay, S.A. (2011). The ELF4-ELF3-LUX complex links the circadian clock to diurnal control of
814   hypocotyl growth. Nature *475*, 398-402.
815   Onai, K., and Ishiura, M. (2005). PHYTOCLOCK 1 encoding a novel GARP protein essential for the
816   Arabidopsis circadian clock. Genes Cells *10*, 963-972.
817   Ouyang, Y., Andersson, C.R., Kondo, T., Golden, S.S., and Johnson, C.H. (1998). Resonating
818   circadian clocks enhance fitness in cyanobacteria. Proc Natl Acad Sci U S A *95*, 8660-8664.
819   Plautz, J.D., Straume, M., Stanewsky, R., Jamison, C.F., Brandes, C., Dowse, H.B., Hall, J.C., and
820   Kay, S.A. (1997). Quantitative Analysis of Drosophila period Gene Transcription in Living
821   Animals. Journal of Biological Rhythms *12*, 204-217.
822   Poire, R., Wiese-Klinkenberg, A., Parent, B., Mielewczik, M., Schurr, U., Tardieu, F., and Walter,
823   A. (2010). Diel time-courses of leaf growth in monocot and dicot species: endogenous rhythms
824   and temperature effects. J Exp Bot *61*, 1751-1759.

825 Pokhilko, A., Fernandez, A.P., Edwards, K.D., Southern, M.M., Halliday, K.J., and Millar, A.J.
826 (2012). The clock gene circuit in Arabidopsis includes a repressilator with additional feedback
827 loops. Mol Syst Biol 8, 574.
828 Pruneda-Paz, J.L., Breton, G., Para, A., and Kay, S.A. (2009). A functional genomics approach
829 reveals CHE as a component of the Arabidopsis circadian clock. Science 323, 1481-1485.
830 Saito, H., Ogiso-Tanaka, E., Okumoto, Y., Yoshitake, Y., Izumi, H., Yokoo, T., Matsubara, K., Hori,
831 K., Yano, M., Inoue, H., et al. (2012). Ef7 encodes an ELF3-like protein and promotes rice
832 flowering by negatively regulating the floral repressor gene Ghd7 under both short- and long-
833 day conditions. Plant Cell Physiol 53, 717-728.
834 Sakuraba, Y., Han, S.H., Yang, H.J., Piao, W., and Paek, N.C. (2016). Mutation of Rice Early
835 Flowering3.1 (OsELF3.1) delays leaf senescence in rice. Plant Mol Biol.
836 Sakuraba, Y., Jeong, J., Kang, M.Y., Kim, J., Paek, N.C., and Choi, G. (2014). Phytochrome-
837 interacting transcription factors PIF4 and PIF5 induce leaf senescence in Arabidopsis. Nat
838 Commun 5, 4636.
839 Schneider, C.A., Rasband, W.S., and Eliceiri, K.W. (2012). NIH Image to ImageJ: 25 years of
840 image analysis. Nat Meth 9, 671-675.
841 Shor, E., and Green, R.M. (2016). The Impact of Domestication on the Circadian Clock. Trends
842 Plant Sci 21, 281-283.
843 Sievers, F., Wilm, A., Dineen, D., Gibson, T.J., Karplus, K., Li, W., Lopez, R., McWilliam, H.,
844 Remmert, M., Soding, J., et al. (2011). Fast, scalable generation of high-quality protein multiple
845 sequence alignments using Clustal Omega. Mol Syst Biol 7, 539.
846 Song, Y.H., Ito, S., and Imaizumi, T. (2010). Similarities in the circadian clock and
847 photoperiodism in plants. Curr Opin Plant Biol 13, 594-603.
848 Song, Y.H., Shim, J.S., Kinmonth-Schultz, H.A., and Imaizumi, T. (2014). Photoperiodic Flowering:
849 Time Measurement Mechanisms in Leaves. Annu Rev Plant Biol.
850 Van Leene, J., Eeckhout, D., Cannoot, B., De Winne, N., Persiau, G., Van De Slijke, E., Vercruysse,
851 L., Dedecker, M., Verkest, A., Vandepoele, K., et al. (2015). An improved toolbox to unravel the
852 plant cellular machinery by tandem affinity purification of Arabidopsis protein complexes. Nat
853 Protocols 10, 169-187.
854 Vizcaino, J.A., Deutsch, E.W., Wang, R., Csordas, A., Reisinger, F., Rios, D., Dianes, J.A., Sun, Z.,
855 Farrah, T., Bandeira, N., et al. (2014). ProteomeXchange provides globally coordinated
856 proteomics data submission and dissemination. Nat Biotechnol 32, 223-226.
857 Wang, L., Si, Y., Dedow, L.K., Shao, Y., Liu, P., and Brutnell, T.P. (2011a). A low-cost library
858 construction protocol and data analysis pipeline for Illumina-based strand-specific multiplex
859 RNA-seq. PLoS One 6, e26426.
860 Wang, W., Barnaby, J.Y., Tada, Y., Li, H., Tor, M., Caldelari, D., Lee, D.U., Fu, X.D., and Dong, X.
861 (2011b). Timing of plant immune responses by a central circadian regulator. Nature 470, 110-
862 114.
863 Wang, Z., Casas-Mollano, J.A., Xu, J., Riethoven, J.J., Zhang, C., and Cerutti, H. (2015). Osmotic
864 stress induces phosphorylation of histone H3 at threonine 3 in pericentromeric regions of
865 Arabidopsis thaliana. Proc Natl Acad Sci U S A 112, 8487-8492.

866 Weller, J.L., Liew, L.C., Hecht, V.F.G., Rajandran, V., Laurie, R.E., Ridge, S., Wenden, B., Vander
867 Schoor, J.K., Jaminon, O., Blassiau, C., *et al.* (2012). A conserved molecular basis for
868 photoperiod adaptation in two temperate legumes. Proc Natl Acad Sci U S A *109*, 21158-21163.
869 Wijnen, H., and Young, M.W. (2006). Interplay of circadian clocks and metabolic rhythms. Annu
870 Rev Genet *40*, 409-448.
871 Woelfle, M.A., Ouyang, Y., Phanvijhitsiri, K., and Johnson, C.H. (2004). The adaptive value of
872 circadian clocks: an experimental assessment in cyanobacteria. Curr Biol *14*, 1481-1486.
873 Wu, J.F., Wang, Y., and Wu, S.H. (2008). Two new clock proteins, LWD1 and LWD2, regulate
874 Arabidopsis photoperiodic flowering. Plant Physiol *148*, 948-959.
875 Yang, Y., Peng, Q., Chen, G.-X., Li, X.-H., and Wu, C.-Y. (2013). OsELF3 is involved in circadian
876 clock regulation for promoting flowering under long-day conditions in rice. Mol Plant *6*, 202-
877 215.
878 Yu, J.W., Rubio, V., Lee, N.Y., Bai, S., Lee, S.Y., Kim, S.S., Liu, L., Zhang, Y., Irigoyen, M.L., Sullivan,
879 J.A., *et al.* (2008). COP1 and ELF3 control circadian function and photoperiodic flowering by
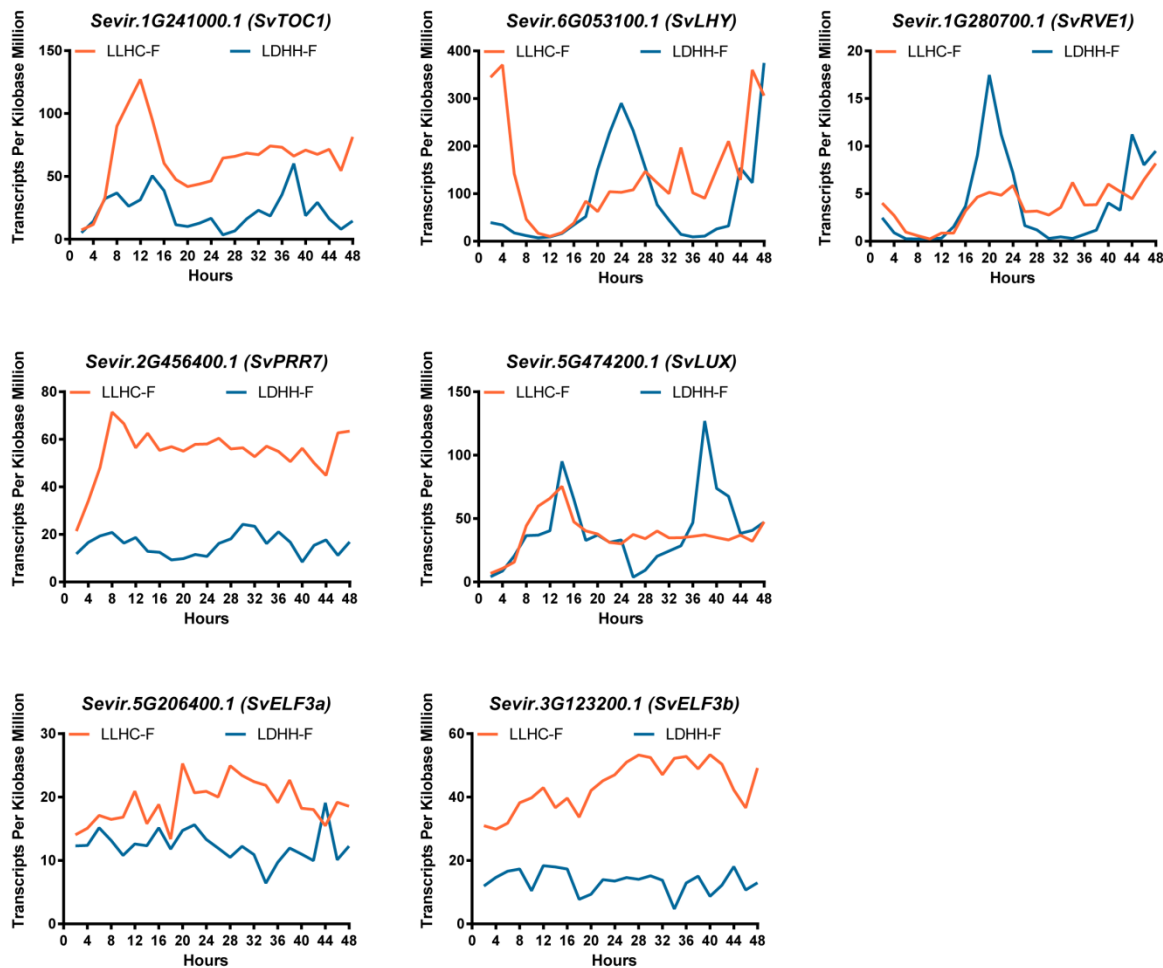880 regulating GI stability. Mol Cell *32*, 617-630.
881 Zagotta, M., Shannon, S., Jacobs, C., and Meeks-Wagner, D. (1992). Early-Flowering Mutants of
882 *Arabidopsis thaliana*. Functional Plant Biology *19*, 411-418.
883 Zakhrabekova, S., Gough, S.P., Braumann, I., Muller, A.H., Lundqvist, J., Ahmann, K., Dockter, C.,
884 Matyszczak, I., Kurowska, M., Druka, A., *et al.* (2012). Induced mutations in circadian clock
885 regulator Mat-a facilitated short-season adaptation and range extension in cultivated barley.
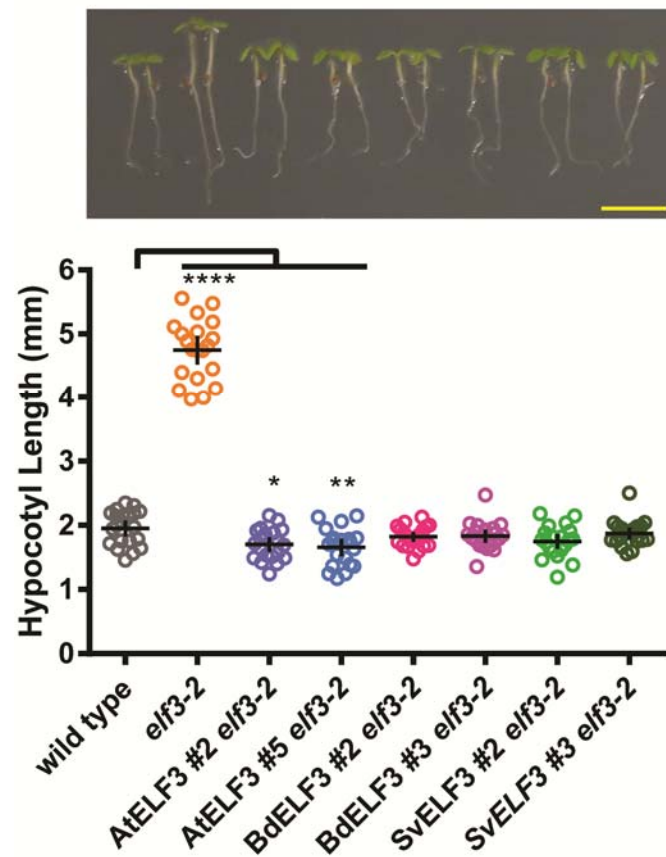886 Proc Natl Acad Sci U S A *109*, 4326-4331.
887 Zhang, X., Henriques, R., Lin, S.-S., Niu, Q.-W., and Chua, N.-H. (2006). Agrobacterium-mediated
888 transformation of Arabidopsis thaliana using the floral dip method. Nat Protocols *1*, 641-646.
889 Zhao, J., Huang, X., Ouyang, X., Chen, W., Du, A., Zhu, L., Wang, S., Deng, X.W., and Li, S. (2012).
890 OsELF3-1, an ortholog of Arabidopsis early flowering 3, regulates rice circadian rhythm and
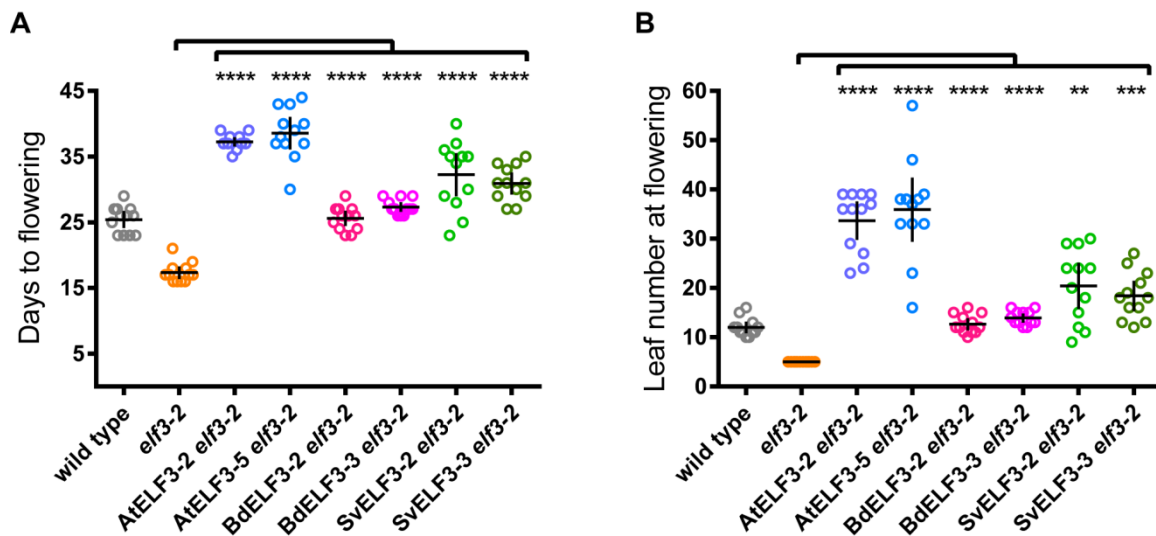891 photoperiodic flowering. PLoS One *7*, e43705.
892 Zhu, D., Maier, A., Lee, J.H., Laubinger, S., Saijo, Y., Wang, H., Qu, L.J., Hoecker, U., and Deng,
893 X.W. (2008). Biochemical characterization of Arabidopsis complexes containing
894 CONSTITUTIVELY PHOTOMORPHOGENIC1 and SUPPRESSOR OF PHYA proteins in light control of
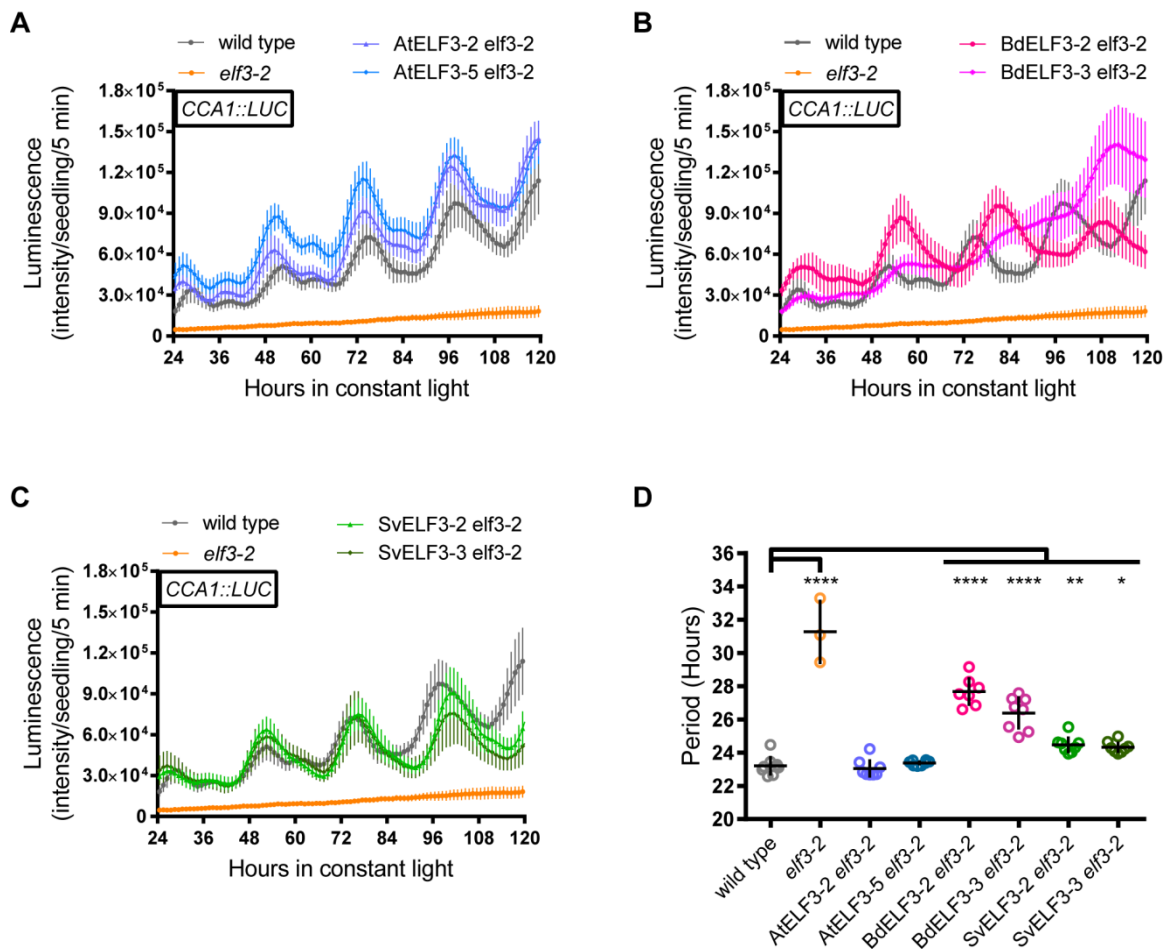895 plant development. Plant Cell *20*, 2307-2323.
896

Figure 1. Circadian expression profiles of putative *S. viridis* clock components from Diel Explorer using time-course RNA-seq data. *S. viridis* plants were entrained by either photocycle (LDHH) or thermocycle (LLHC), followed by being sampled every 2 hours for 48 hours under constant temperature and light conditions (Free-Running; F) to generate time-course RNA-seq data. Mean values of Transcripts per Kilobase Million (TPM) from two experimental replicates for each timepoints per gene were plotted.
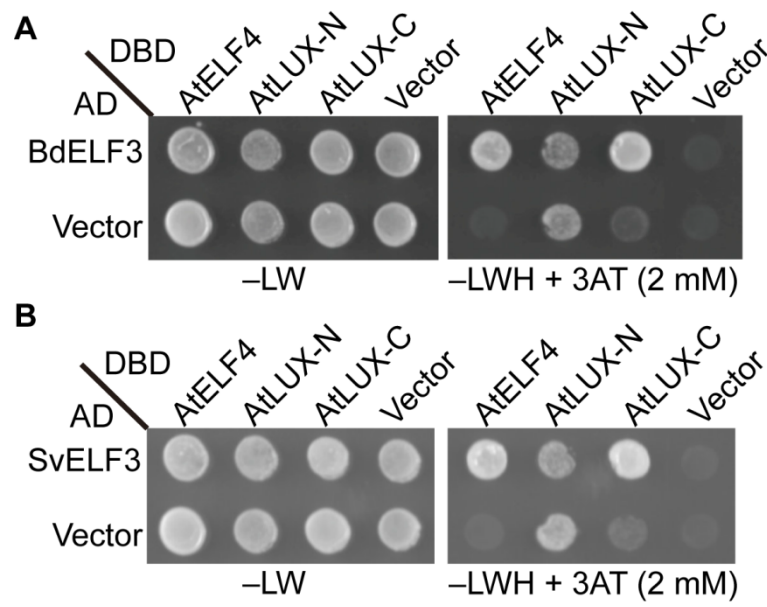
Figure 2. ELF3 orthologs suppress hypocotyl elongation defects in *elf3-2*. The hypocotyls of 20 seedlings of wild type, *elf3-2* mutant, AtELF3 *elf3-2*, BdELF3 *elf3-2*, and SvELF3 *elf3-2* (two independent transgenic lines for each ELF3 ortholog) were measured at 4 days after germination under 12-hour light :12-hour dark growth conditions at 22 ˚C. Upper panel shows representative seedlings of each genotype, with scale bar equal to 5 mm. Mean and 95% confidence intervals are plotted as crosshairs. This experiment was repeated three times with similar results. ANOVA analysis with Bonferroni correction was used to generate adjusted P values, $* < 0.05$, $** < 0.01$, $**** < 0.0001$.

Figure 3. ELF3 orthologs suppress time to flowering of *elf3-2*. 12 wild type, *elf3-2* mutant, AtELF3 *elf3-2*, BdELF3 *elf3-2*, and SvELF3 *elf3-2* seedlings from two independent transformations were measured for days **(A)** and number of rosette leaves **(B)** at flowering (1 cm inflorescence). Mean and 95% confidence intervals are plotted as crosshairs. This experiment was repeated twice with similar results. ANOVA analysis with Bonferroni correction was used to generate adjusted P values, ** < 0.01, *** < 0.001, **** < 0.0001, of measurements when compared to the *elf3-2* mutant line.

Figure 4. ELF3 orthologs can recover *CCA1::LUC* rhythms and amplitude in *elf3-2* mutants. 8 seedlings of wild type, *elf3-2* mutant, AtELF3 *elf3-2* **(A)**, BdELF3 *elf3-2* **(B)**, and SvELF3 *elf3-2* **(C)** from two independent transformations were imaged for bioluminescence under constant light after entrainment in 12-hour light :12-hour dark growth conditions at 22 ˚C. Each plot shows average bioluminescence of all seedlings along with 95% confidence interval (error bars). This experiment was repeated four times with similar results. Note that wild type and *elf3-2* mutant data was plotted on all graphs for comparison. **(D)** Periods of seedlings. Only periods with a Relative Amplitude Error below 0.5 (see **Supplemental Figure S7**) were plotted. Mean and 95% confidence intervals are plotted as crosshairs. ANOVA analysis with Bonferroni correction was used to generate adjusted P values, $* < 0.05$, $** < 0.01$, $*** < 0.001$, $**** < 0.0001$, of measurements when compared to the wild type.

Figure 5. Both BdELF3 and SvELF3 can directly bind to AtELF4 and AtLUX. Yeast two-hybrid analysis of testing if either BdELF3 **(A)** or SvELF3 **(B)** can directly interact with either AtELF4, the N-terminal half of AtLUX (AtLUX-N, a.a. 1-143) or the C-terminal half of AtLUX (AtLUX-C, a.a. 144-324). –LW tests for the presence of both bait (DBD) and pray (AD) vectors, while the –LWH + 3AT tests for interaction. Vector alone serves as interaction control. This experiment was repeated twice with similar results.